



Dynamic nanoindentation of articular porcine cartilage

O. Franke^{a,c}, M. Göken^a, M.A. Meyers^b, K. Durst^a, A.M. Hodge^{c,*}

^a Department of Material Science and Engineering, University Erlangen-Nuremberg, Germany

^b Department of Mechanical and Aerospace Engineering, University of California, San Diego, CA, USA

^c Department of Aerospace and Mechanical Engineering, University of Southern California, Los Angeles, CA, USA

ARTICLE INFO

Article history:

Received 14 April 2010

Received in revised form 7 December 2010

Accepted 17 December 2010

Available online 28 December 2010

Keywords:

Articular cartilage

Biological materials

Indentation

Time-dependent mechanical properties

Storage and loss modulus

Dynamic nanoindentation

ABSTRACT

Articular cartilage is a poroelastic (biphasic) material with a complex deformation behavior, which can be considered elastic–viscoelastic. In this article, articular porcine cartilage is tested *in vitro* using dynamic nanoindentation and is analyzed using the frequency domain. The testing and data analysis are presented as a function of the strain rate and frequency, which allows for the results to be compared for various load amplitudes over the same frequency range. In addition, a new approach to correct the contact area during dynamic nanoindentation is presented and the effects of sample freezing on the mechanical properties are also discussed.

© 2011 Elsevier B.V. All rights reserved.

1. Introduction

Cartilage, and especially articular, cartilage is an important subject for biomechanical studies [1–13]. Its function is extremely important for the mobility and the operation of joints, and unlike most other human tissue, it is not innervated [3,14,15] and therefore presents no early warning signals to damage. Once the tissue is damaged (as in the case of osteoarthritis [6,14,16]), it has to be either replaced or repaired [17–19]. Hence, it is crucial to understand its biochemical as well as its mechanical properties in order to generate biomimetic materials of similar quality [4–6,12,17,18,20,21].

In general, quasistatic testing provides a valuable insight in the mechanical properties and allows for analysis of different repair tissues [4–6,12,17,18,20,21], although it cannot directly capture the dynamic, time-dependent properties. Currently, quasistatic testing is implemented *in vivo* and can be used by a surgeon to measure the stiffness of the tissue during a procedure using an arthroscope (for instance, load relaxation [21]). However, the results are hard to quantify and highly dependent on the surgeon's test approach. In the case of time-dependent behavior, tests are currently only performed *in vitro* using one of the two available methods. These methods are (a) the time-space method for which one can use a creep experiment and appraise the response to a constant load for a given time [22–26] or use load relaxation [21] and (b) the frequency space method, for which the tests are performed at varying frequencies [22,27–29]. In the frequency space

methodology, macro-DMA techniques apply a pre-load to the whole sample and oscillate at a given frequency [10], while other tests can be performed on a more local scale using macroscopic indenters [1,11]. For example, Young et al. studied the dynamic behavior in respect to the Mankin score (a score to evaluate the quality of tissue based on histology and structural aspects) using a handheld device [13], while the work by Tanaka et al. was performed with a custom-made machine at different locations and frequencies, yielding an increase in the storage modulus for mandibular condylar cartilage from 0.1 MPa to almost 1.5 MPa in the range of 0.01–10 Hz [11].

In this study, dynamic nanoindentation is evaluated as a technique to test articular cartilage in the frequency range of 1–250 Hz. These frequencies were chosen because of their relevance to actual loading conditions encountered during regular gait [30]. The technique was selected based on the capability of nanoindentation to produce quantifiable and reproducible results with a high lateral resolution. Specific prerequisites for accurate dynamic testing at the nanoscale as described by Asif et al. [27] have been taken into account. In addition, a new method is suggested to determine the projected contact area using a sharp indenter for the analysis of viscoelastic materials. Furthermore, the effects of fresh and frozen tissue on such measurements are discussed.

2. Materials and methods

2.1. Specimen selection and preparation

The tissue samples were obtained from Sierra Medical Inc., Sylmar, CA, and dissected directly upon arrival using a miniature

* Corresponding author. Department of Aerospace and Mechanical Engineering, University of Southern California, Los Angeles, CA, USA.

E-mail address: ahodge@usc.edu (A.M. Hodge).

rotating saw to obtain cubic samples with a side length of about 4–5 mm. The pigs were 5–7 months old and used for meat production. The time between the sacrifice of the animal and the delivery was between 1 and 2 h with the samples being cooled the entire time. All samples were taken from the center of the patella. The patella was chosen because of its easy availability, high homogeneity throughout, and its high importance for medical research. The tests were performed perpendicular to the native surface within the upper zone of the tissue. Since the surface is fairly smooth, no further sample preparation was applied. For these type of samples, the surface roughness was determined by Park et al. to be $\sim 462 \pm 216$ nm in a scan area of $100 \times 100 \mu\text{m}$ [31]. A study by Patel et al. determined a value of 95.4 ± 28.0 nm to 130.1 ± 13.8 nm [32].

Given the size of the indent at a displacement of $3 \mu\text{m}$, the influence on the indentation can be neglected. The test locations were carefully selected to ensure that the surface was smooth enough for indentation testing and the indents were performed in the center of the specimen to limit the influence of damage caused by cutting the samples. The subchondral bone was not removed and used to glue the samples into small plastic containers, thus guaranteeing a mechanically stable foundation. The glue cannot affect the tested surface, since no contamination can occur through the bone and the tissue. After the samples were placed in the container, the samples were hydrated with phosphate-buffered saline [17,18,33]. No significant swelling was observed as the samples were kept moist at all times. The use of a liquid tip with a longer shaft allowed for the tissue to be submerged under a liquid film of 2–3 mm at all times, thus maintaining a constant environment throughout the whole test. Samples analyzed within the first 24 h after the death of the animal are referred to as fresh, while samples that were frozen either during transport or due to storage are referred to as frozen. Multiple single frequency and frequency sweep tests were performed in up to three tissue samples for each condition (fresh or frozen). More specifically, for the single frequency tests, at least three individual tests were performed per sample at a specific frequency. These set of tests were performed on randomly chosen areas of the sample, which met the required surface criterion. For the frequency sweeps, up to seven tests were performed on each sample.

In order to maintain a damage-free sample surface for the SEM-imaging, all samples were critical point dried. As a first step, the PBS is replaced by ethanol in an increasing series of ethanol concentration (from 10%, 30%, 50%, 70%, 90% to 100%) where the sample is soaked for 5 min in each solution. Ethanol was chosen because of its lower surface tension than water, which facilitates the substitution by CO_2 in the critical point drying process. Furthermore, the gas flow was closely monitored throughout the critical point drying and the samples were coated with a thin AuPd-layer upon completion of the drying using an evaporation technique. All imaging was performed in a FEI-XL30 SEM (FEI Company, OR).

2.2. Dynamic nanoindentation

In dynamic nanoindentation, an oscillation is superimposed on the regular load signal, thus, providing a continuous measurement of the modulus during an experiment also known as continuous stiffness measurement as first described by Oliver and Pharr [34]. For this purpose, the machine was calibrated using both quasistatic and dynamic calibration techniques, which were performed in liquid to eliminate the influence of any additional damping. For the dynamic calibration, the machine response was monitored between 10 and 250 Hz.

Several load profiles were used in this work. The first load profile is a frequency sweep carried out between 10 and 250 Hz (made up of 25 equally spaced frequency steps with 100 cycles each). All the applied load sets and the corresponding frequencies are given in Table 1. The second load profile is the ramp load, where the quasistatic load is

Table 1
Load Profiles used in this study

Profile	Quasistatic loads in μN	Dynamic load amplitudes in μN	Frequencies in Hz
Ramping load	100–1000	1.0 and 2.0	10
Frequency sweep	1000	1.0 and 2.0	10–250
Constant	1000	1.0 and 2.0	1, 2.5, 5, 7.5, 10, 20

increased while the frequency and the dynamic load stay constant. This profile has the advantage of having a fast loading segment (loading rates $> 100 \mu\text{N/s}$) so that the projected contact area can be obtained from the tip area function, since viscoelastic flow will be negligible when the sample is loaded fast enough. Thus, the contact stiffness and more importantly the contact area can be determined using the tip area function as described by Oliver and Pharr [34]. The third profile is the constant profile, which is a mixture of the previous profiles. This load profile allows for each value to be averaged over up to 15 segments with 100 cycles each. All three testing parameters (static load, dynamic load, and frequency) are kept constant throughout the entire test. Each value shown for the single frequency tests is an average of at least 1200 cycles for up to 9 indents (three locations on up to three samples). For the frequency sweeps, each data point is an average over 100 cycles and each sweep has been repeated several times in different sample areas (up to seven per sample) and on different samples.

During the dynamic indentation of a sample, given that the material is not in resonance, a phase shift between the applied and the measured response signal will be observed. This phase shift is the signal that was originally used by Oliver and Pharr to determine the reduced modulus of the sample [34]. However, when a material exhibits a time-dependent behavior, it is necessary to adapt the model to accommodate this behavior since the phase shift can no longer be attributed solely to the reduced modulus. In practice, the time-dependent deformation is captured by adding a dashpot to the model representing the experimental setup where the dashpot can describe a delayed mechanical response. There are several ways of aligning the dashpot, which are widely discussed in literature such as for instance the linear viscoelastic solid or the Kelvin model. In this work, the so-called Kelvin solid was used where the sample is represented by a parallel alignment of a dashpot and a spring. This model is limited in its ability to describe a purely elastic response. Nonetheless, it is considered the state of the art model for dynamic indentation since its main advantage is the calibration procedure, which requires few assumptions and is well understood. The mechanical response can thus be divided into two parts: the storage modulus E' and the loss modulus E'' . These two moduli can be described as a complex modulus E^* (Eq. (1)) with the phase angle δ being the angle between the real axis and the vector representing the complex modulus in a phasor diagram. While the storage modulus is the real part of the complex modulus, the loss modulus is equivalent to the imaginary part.

$$E^* = E' + iE'' \quad (1)$$

E' describes the in phase elastic response of a given material (Eq. (2)), and E'' is a measure for the damping/energy being dissipated throughout the experiment (Eq. (3)). We note at this point that the use of the Sneddon equation is limited to elastic and linear viscoelastic materials only. However, since each frequency is evaluated separately, it can be assumed that the Kelvin model can provide a reasonable approximation. The following equations (Eqs. (2–4)) are the basic expressions used in dynamic nanoindentation to determine the

storage and loss modulus and the loss factor, from the machine output values (similar to Refs. [28,35,36]).

$$E' = \frac{S\sqrt{\pi}}{2\sqrt{A_c}} \quad (2)$$

$$E'' = \frac{\omega D_c \sqrt{\pi}}{2\sqrt{A_c}} \quad (3)$$

$$\tan\delta = \frac{E''}{E'} = \frac{D_c \omega}{S} \quad (4)$$

where S is the contact stiffness, ω is frequency, A_c is projected contact area, and D_c is contact damping.

3. Results and discussion

In the initial stage of this study, frozen cartilage samples were tested in comparison to fresh samples. In earlier studies [37], at large displacements, no influence of freezing on the reduced modulus was observed; however, a change in the contact stiffness was observed. Since the dynamic nanoindentation was only carried out in the superficial zone due to the displacement limitations of the testing equipment, it is more sensitive to changes in the surface. Furthermore, dynamic nanoindentation also has a higher resolution, which can be used to enlighten effects such as freezing. It can clearly be seen that the moduli are lower for the frozen tissue sample (Fig. 1). This reduction in modulus is due to the damage in the tissue caused by the uncontrolled freezing of the tissue. The most likely cause for this damage is a crystallization of the water, which leads to a rupture of the fibers near the surface, which is enhanced by the fact that the tissue is surrounded by synovial fluid. In critical point dried tissue samples, the damaged surface is visible in the SEM as the tissue is preserved in its original condition throughout the drying process. While the fresh tissue has a smooth surface (Fig. 2a and c), the frozen tissue exhibits spongy extrusions with obvious ruptures of the tissue in the vicinity of the extrusions (Fig. 2b and d). This damage is not only limited to the visible surface, but most likely causes a 3D rupture of the tissue. Therefore, only fresh tissues are used for the rest of this study.

In Fig. 3, the storage and loss modulus are shown for the tests run on three different fresh samples with up to three tests on each sample. The standard deviation denoted is the average deviation of all the tests performed for a given set of parameters. There is a slight increase in the variance of the tests with increasing time, which is the reason for the testing time constraint [17,18,37]. The values compare well with previous studies on articular cartilage of the patella (Göttingen minipig) using quasistatic indentation and a Berkovich indenter,

where a value of 2.5 ± 0.7 MPa was determined [17,18,33,37]. A macroscopic study by Demarteau et al. found the Young's modulus to vary from 1.64 ± 0.34 MPa for human to 0.28 ± 0.14 MPa for bovine femoral cartilage [38].

Typical tests on soft biological materials and polymers use a flat punch as an indenter since it provides a constant contact area independent of the displacement [22,28,39–41]. The selection of the right punch size requires prior knowledge of the materials behavior and the contact of a flat punch is not self-similar with unknown edge effects influencing the results. In this study, a Berkovich tip was used given that its large opening angle limits the damage to the tissue [17,18,33,37] and the contribution of the edges is relatively small compared to the contact provided by the sides [17,18,33,37]. Another benefit of this tip selection is the self-similarity of the tip and the resulting stress field around the tip [42].

Given the arguments above and following the reasoning of earlier studies on cartilage, and other viscous materials, a Berkovich indenter was chosen as a good fit for this study [17,18,24,33,37,43]. However, using a Berkovich tip can provide some inaccuracies in the area determination, which can significantly influence the results; thus, in order to access this effect, the following tip area correction is proposed and evaluated.

3.1. Tip area correction

In Fig. 4, the storage modulus and the loss modulus are shown for one set of tests performed at different frequencies between 1 and 20 Hz using a modified tip area function and compared to unmodified values. The tip area correction was performed for all tests except for the 10 Hz test, which was the reference frequency. For the uncorrected values, there is an obvious increase for the storage modulus from 3.6 ± 0.3 MPa at 1 Hz to 8.8 ± 0.2 MPa at 20 Hz. Besides showing a stiffer mechanical response, the tissue is also damping more and dissipating more energy as the loss modulus increases from 2.2 ± 0.2 MPa to 4.2 ± 0.2 MPa in the same frequency range. Even though the slope is decreasing, there is no clear sign for a plateau or saturation being reached at 20 Hz. The area correction lowers the modulus values (since the contact area is usually underestimated) while maintaining the trend of the frequency dependencies. Thus, the storage modulus at 1 Hz is 3.1 ± 0.1 MPa and increases to 7.5 ± 0.2 MPa at 20 Hz. The trend is the same for the loss modulus; however, the absolute change is not the same as the moduli do not scale linearly with the change in the contact area. Thus the loss modulus is 1.9 ± 0.1 MPa at 1 Hz and 3.5 ± 0.2 MPa at 20 Hz. By using the proposed correction, it was found that the values obtained for the correction varied between 25% and 40% and thus match well with the ones observed by Deuschle et al. [44] for *in situ* experiments. The same procedure was carried out on N-Butadien Rubber (NBR) and let to comparable (reduction of E' from 23 MPa to 15 MPa at 1 Hz) results to flat punch indentation and to literature values from macroscopic room temperature experiments [37,45,46].

The correction for the change in contact is as shown in Fig. 5a–c, by using a combination of the ramp load and constant profile (Fig. 5d). The change in the contact is mainly caused by creep and adhesion causing a pile-up formation around the indenter. Even though no plastic deformation was observed, there are other deformation mechanisms in a biomaterial such as viscoelasticity and viscoplasticity that could cause a pile-up like behavior around the indenter even though no permanent deformation is observed. The proposed correction is comparable to a pile-up correction in hardness measurements but does not specify a certain contact geometry, meaning that a correction for either a pile-up or for a stronger than predicted sink-in can be made. Unlike for pile-up corrected hardness, the modulus is not taken from literature but from the measurement in the ramp load. The reference moduli are determined as a function of the displacement measured by the system at the reference frequency

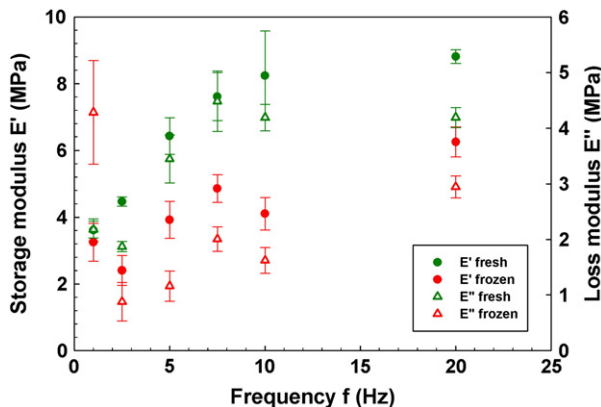


Fig. 1. Storage and loss modulus of a fresh and a frozen sample in direct comparison. Note the two different y-axis scales for loss and storage modulus.

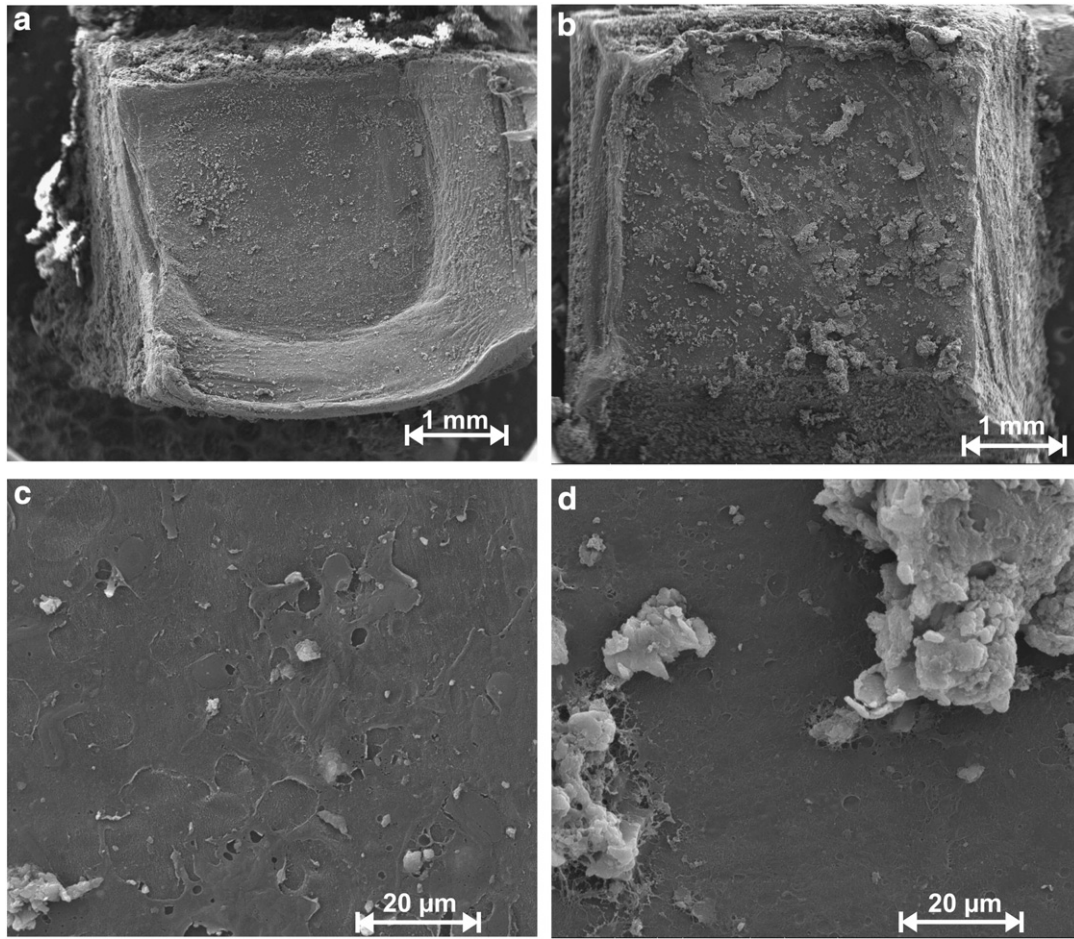


Fig 2. SEM micrographs of the surface of a critical point dried sample in the fresh condition at two different magnifications (a and c) and of a frozen sample at high and low magnifications (b and d). Note the spongy extrusions on the frozen sample caused by a freeze-burn-like mechanism.

and thus provide an internal calibration of the tip area, which is then used to correct the contact area. This is important since the contact evolves as a consequence of the loading parameters, duration of the experiment and material, thus the contact geometry is unique to each set of those parameters. For instance, a lower than expected modulus for the second reference measurement must be caused by a change in the contact area namely an increase in the contact area. In this study, the values shown in Fig. 4 led to the conclusion that the change in contact is similar to a pile-up, since the correction showed that the contact area was underestimated.

When a constant profile test at the reference frequency (for instance, 10 Hz) is performed after a test at another frequency (for instance 5 Hz) and yields a different value for the reference modulus, this change can be attributed to a change in contact area. While this change might be small under some circumstances, it can amount to a significant value as reported by Deuschle et al. [44]. Thus, the contact area will be determined from the reference measurement, and the values obtained for the test frequency can be corrected with the newly acquired contact area. The load profile necessary for the correction is

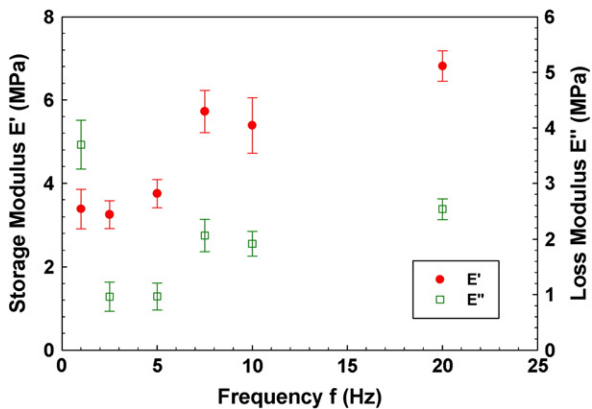


Fig. 3. Storage and the loss modulus for all single frequency tests performed in this study. Note the two different y-axis scales for loss and storage modulus.

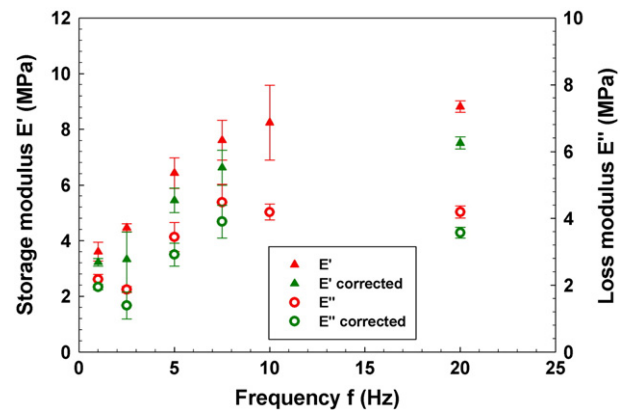


Fig 4. Representative corrected and uncorrected storage and loss modulus results for tests on one hyaline cartilage sample. Note the two different y-axis scales for loss and storage modulus.

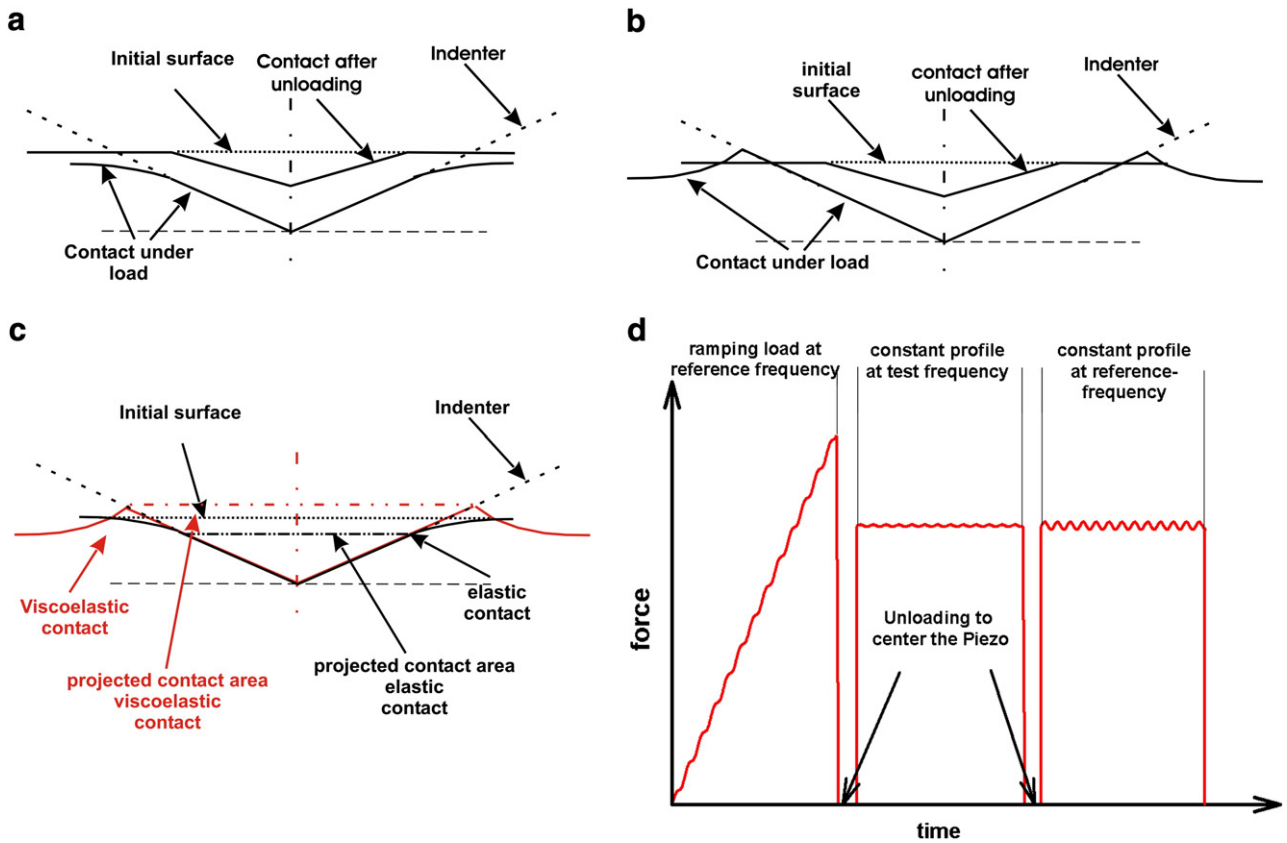


Fig. 5. Possible contact configurations as found during nanoindentation, (a) sink-in behavior as described in the Oliver–Pharr method, which occurs for a lot of elastic–plastic materials such as alloys, (b) pile-up behavior as to be expected, for example, in some metals and viscoelastic materials. Note that the contact geometry after unloading refers to a state where no significant inelastic recovery has yet occurred. For some viscoelastic materials (such as the cartilage in this study), low loads do not cause any visible deformation after a certain recovery time. (c) A comparison of the projected contact areas for the viscoelastic and the elastic–plastic contact. The projected contact area as calculated from the tip-area function (black line for elastic–plastic-contact in the picture) underestimates the viscoelastic contact with a pile-up (red line) and (d) load profile required to perform the internal calibration of the projected contact area consisting of three steps.

shown in Fig. 5d. For the application of this technique, the following assumptions are made:

- The modulus is constant for a certain frequency at a given displacement (in this study, 10 Hz and displacements between 2.5 and 3 μm were used).
- The projected contact area obtained from the calibrated tip area function is valid for fast loading as used in the ramp load.

The first assumption is the basis of all dynamic tests and was validated by performing verification runs in all tested samples. Furthermore, the load for the constant profiles was chosen so that all tests were in a regime with constant storage and loss modulus regarding the total displacement at this point. The second assumption is valid in so far as all effects influencing the indenter–sample contact are time-dependent and thus negligible on a short time scale. The influence of the pile-up is time-dependent and thus more dominant for slow experiments at low frequencies or if long settling times are required for the system to stabilize. While the settling time can be minimized by allowing for enough time in the stabilization of the machine (so that it is steady before the actual indent), the testing at low frequencies of less than 5 Hz is more volatile to this effect. A classical time frame for the total experiment is several minutes with the longest individual test consisting of 1500 cycles at 1 Hz.

At this point, it should be noted that in this work, pull-off force experiments were performed and it was concluded that the contribution of the adhesion force on the dynamic in vitro tests was negligible since all tests were performed inside a liquid (PBS), which suppressed adhesion effects.

3.2. Strain-rate effects

As previously discussed, the joints undergo a variety of loading conditions at a wide range of frequencies; thus, frequencies from 10 to 250 Hz were tested. To vary the strain rate, the frequency and also the dynamic load were varied during the tests. As shown by Mayo et al. [47], the loading rate is proportional to the strain rate for materials with a displacement and time-independent hardness; however, there are two prerequisites to be met. The first one is a constant modulus for a certain frequency at a given displacement, which is easily achieved in dynamic nanoindentation since the displacement in the experiment is limited as compared to quasistatic testing. Even though cartilage has a complex structure, given the small oscillatory displacement in the submicron regime, the structure, and consequently the resulting modulus can be considered as displacement independent. The second assumption requires a constant hardness and is difficult to verify for viscoelastic materials. However, in the time-frame used for this study, no changes in the contact pressure as a consequence of a preconditioning are to be expected. Even at larger displacements using several load–unload cycles, no significant effect could be found.

The plot of the moduli as a function of the frequency shows no clear trend for the varying dynamic loads (Fig. 6a and b). However, the influence can clearly be distinguished if (\dot{P}/P) is plotted where \dot{P} denotes the dynamic loading rate and P the total applied load (Fig. 6c). In the frequency plot, only the storage modulus for a dynamic load of 1 μN seems to show a plateau region, which cannot be distinguished for the 2 μN tests. Tests were also run at a dynamic load of 0.5 μN , but

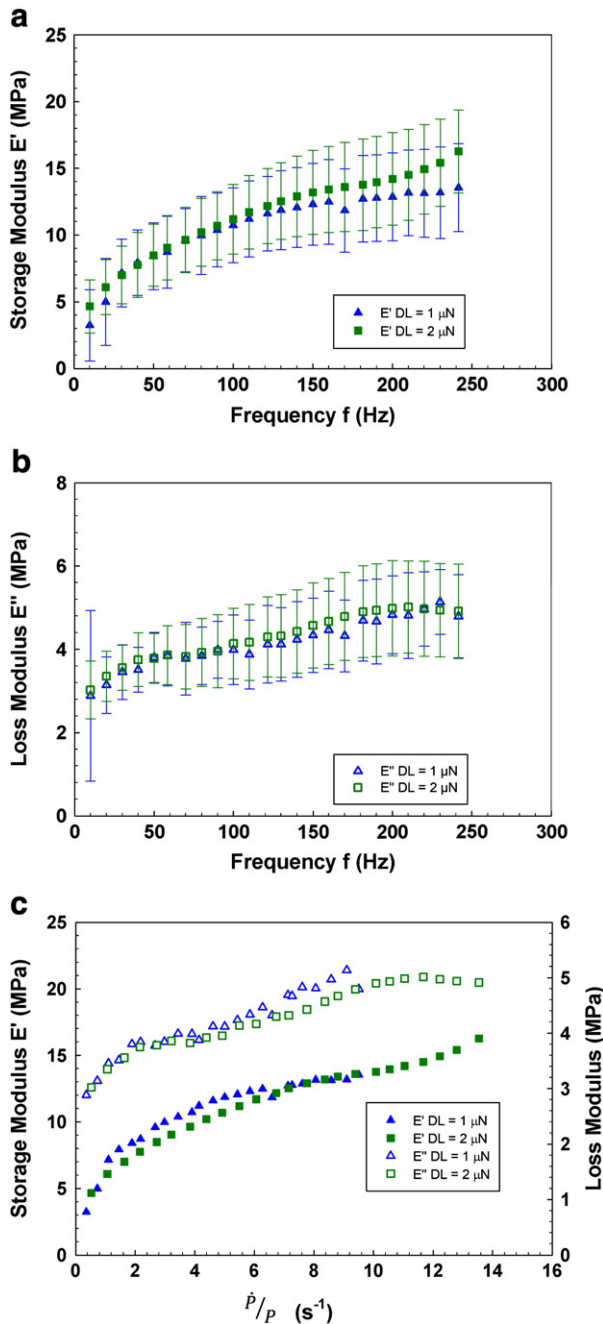


Fig 6. Corrected storage and loss modulus as obtained by a frequency sweep between 10 and 250 Hz shown as a function of the frequency (a and b) and (c) Normalized loading rate for two different dynamic loads. Note the two different y-axis scales for loss and storage modulus in (c).

the resulting dynamic displacement was too low to yield significant results.

Overall the loss modulus steadily increases within the regular scatter. Considering only the two higher dynamic load amplitudes (which are more likely to give a stable result due to the higher magnitude of the resulting signal), higher moduli for higher dynamic load amplitudes are measured. This trend is not very pronounced and could also be considered an artifact, as its magnitude is well within the standard deviation of the experiment. However, it can clearly be seen that all tests have one trend in common: both storage and loss modulus increase over the whole spectrum. If the data are analyzed as a function of the normalized loading rate, which is proportional to the strain rate for a constant hardness/contact pressure, the data for a

dynamic load of 1 μN and 2 μN form a master curve which clearly highlights (1) the limits of the comparability between data plotted as a function of the frequency and (2) the fact that the tested tissue sample may not be considered linear viscoelastic in the tested frequency regime after all. The newly obtained curve seems to be a good test for linear viscoelasticity, since there should only be strong frequency dependence in the moduli. However, it shows the expected intermediate section for the storage modulus with only a slight increase over a wide range of strain rates (in the strain rate range of 6–12 s^{-1}). The loss modulus shows two slopes with a short intermediate section with very little change and levels out towards higher strain rates. This might indicate that there is maximum ability of the tissue to dampen a shock or that a further increase cannot be resolved with the system due to a change in the contact.

4. Conclusion

The main objective of this study was to determine the dynamic response of articular porcine cartilage in the frequency space. All frequencies tested in this study are of high relevance for regular gait, and the results are thus important for our understanding of the mechanical behavior of tissue. The implementation of the models needs further attention, especially when they are applied to a complex system such as in vitro testing of tissue. As a further step, a new approach was introduced to correct for the inaccuracy of the tip area determination in a viscoelastic solid when a sharp indenter is used. This technique enables the user to correct for inaccuracies using an approach similar to the pile-up correction. As a result, the underestimated projected contact area could be corrected, thus, yielding lower values for storage and loss modulus. Furthermore, it could be shown that dynamic nanoindentation has the resolution to accurately measure the influence of surface damage such as freezing.

In dynamic nanoindentation, results are usually shown as a function of the frequency independent of the viscoelastic behavior of the material (linear or not). However, those plots may not always show the effects caused by varying parameters such as the static load or the dynamic load. In order to compare results acquired under different conditions, an analysis as a function of the strain rate is proposed highlighting the influence of the testing parameters on the measured viscoelastic response.

Acknowledgments

The authors (O.F., M.G., and K.D.) would like to acknowledge the financial support by the DFG (Grant: GO741/13-1) and the funding from the German Research Council (DFG), which, within the framework of its “Excellence Initiative,” supports the Cluster of Excellence at the University of Erlangen-Nuremberg. Furthermore, helpful discussions on the testing with S.S. Asif, M. Dickinson, and L. Kuhn (all Hysitron Inc., Minneapolis, MN) are highly appreciated. The SEM images were obtained at Scripps Institute of Oceanography, La Jolla, CA. The authors would like to thank Evelyn York and Dr. Po-Yu Chen (UCSD) for their help in this endeavor. The discussions on literature with Prof. R. Sah and Dr. W. Bae (UCSD) are also acknowledged.

References

- [1] W.C. Hayes, L.F. Mockros, *J. Appl. Physiol* 31 (1971) 562.
- [2] W.C. Bae, et al., *Arthritis Rheum.* 48 (2003) 3382.
- [3] L.C. Dijkgraaf, L.G.M. de Bont, G. Boering, R.S.B. Liem, *J. Oral Maxillofac. Surg.* 53 (1995) 924.
- [4] Ebenstein, D. M. et al. A nanoindentation technique for functional evaluation of cartilage repair tissue. *Journal of Materials Research* 19, 273–281, doi:10.1557/JMR.2004.0031 (2004).
- [5] H.S. Gupta, et al., *J. Struct. Biol.* 149 (2005) 138.
- [6] A. Lau, M.L. Oyen, R.W. Kent, D. Murakami, T. Torigaki, *Acta Biomater.* 4 (2008) 97.
- [7] J.M. Mattice, A.G. Lau, M.L. Oyen, R.W. Kent, Spherical indentation load-relaxation of soft biological tissues, *Journal of Materials Research*, 21, 2003–2010, doi:10.1557/JMR.2006.0243 (2006).

- [8] V.C. Mow, M.C. Gibbs, W.M. Lai, W.B. Zhu, K.A. Athanasiou, Numerical algorithm experimental study, *J. Biomech.* 22 (1989) 853.
- [9] V.C. Mow, M.H. Holmes, W. Michael Lai, *J. Biomech.* 17 (1984) 377.
- [10] S. Park, C.T. Hung, G.A. Ateshian, *Osteoarthritis Cartilage* 12 (2004) 65.
- [11] E. Tanaka, et al., Dynamic compressive properties of the mandibular condylar cartilage, *Journal of Dental Research*, 85, 2006, doi:10.1177/154405910608500618.
- [12] S. Tomkoria, R.V. Patel, J.J. Mao, *Med. Eng. Phys.* 26 (2004) 815.
- [13] A.A. Young, R.C. Appleyard, M.M. Smith, J. Melrose, C.B. Little, *Clinical Orthopaedics and Related Research* 462 (2007) 212.
- [14] T. Hardingham, M. Bayliss, *Semin. Arthritis Rheum.* 20 (1990) 12.
- [15] H. MANKIN, V.C. MOW, J.A. BUCKWALTER, J.P. IANNOTTI, A. RATCLIFFE, *Orthop. Basic Sci.* (2000) 443.
- [16] P.M. van der Kraan, W.B. van den Berg, *Ageing Res. Rev.* 7 (2008) 106.
- [17] O. Franke, et al., *Acta Biomater.* 3 (2007) 873.
- [18] K. Gelse, et al., *Arthritis Rheum.* 58 (2008) 475.
- [19] E.B. Hunziker, Review current status prospects. *Osteoarthritis cartilage* 10 (2002) 432.
- [20] X. Li, et al., Microindentation test for assessing the mechanical properties of cartilaginous tissues, *J Biomed Mater Res Part B: Appl Biomater*, 80B, 2007.
- [21] A.I.N. Vasara, T. Miiika, Jukka S Jurvelin, Lars Peterson, Anders Lindahl, Ilkka Kiviranta, *Clin. Orthop. Relat. Res.* 433 (2005) 233.
- [22] E.G. Herbert, W.C. Oliver, A. Lumsdaine, G.M. Pharr, *J. Mater. Res.* 24 (2009) 626.
- [23] M.L. Oyen, *Acta Mater.* 55 (2007) 3633.
- [24] M.L. Oyen, *J. Mater. Res.* 20 (2005) 2094, doi:10.1557/JMR.2005.0259.
- [25] M.R. VanLandingham, *J. Res. Natl. Inst. Stand. Technol.* 108 (2003) 249.
- [26] M.R. VanLandingham, N.K. Chang, P.L. Drzal, C.C. White, S.H. Chang, I. Quasi static testing. *J. Polym. Sci. B Polym. Phys.* 43 (2005) 1794.
- [27] S.A.S. Asif, K.J. Wahl, R.J. Colton, *Rev. Sci. Instrum.* 70 (1999) 2408.
- [28] E.G. Herbert, W.C. Oliver, G.M. Pharr, *J. Phys. D Appl. Phys.* 41 (2008) 074021.
- [29] G.M. Odegard, T.S. Gates, H.M. Herring, *Exp. Mech.* 45 (2005) 130, doi:10.1007/BF02428185.
- [30] K.A. Gillespie, J.P. Dickey, *Clin. Biomech.* 18 (2003) 50.
- [31] S. Park, K.D. Costa, G.A. Ateshian, *J. Biomech.* 37 (2004) 1679.
- [32] R.V. Patel, J.J. Mao, *Front. Biosci.* 8 (2003) a18.
- [33] O. Franke, M. Göken, A. Hodge, *JOM* 60 (2008) 49.
- [34] W.C. Oliver, G.M. Pharr, *J. Mater. Res.* 7 (1992) 1564.
- [35] S. Asif, K. Wahl, R. Colton, O. Warren, Quantitative imaging of nanoscale mechanical properties using hybrid nanoindentation and force modulation, *Journal of Applied Physics*, 90, 2001.
- [36] I. Hysitron, *TribolIndenter nanoDMA™ User Manual*, 2007.
- [37] Franke, O. *Nanomechanische Eigenschaften hierarchischer Strukturen* Dr.-Ing. thesis, Friedrich-Alexander-Universität Erlangen-Nürnberg, (2009).
- [38] O. Démarteau, L. Pillet, A. Inaebnit, O. Borens, T.M. Quinn, *Osteoarthritis Cartilage* 14 (2006) 589.
- [39] Y. Cao, D. Ma, D. Raabe, *Acta Biomater.* 5 (2009) 240.
- [40] D.M. Ebenstein, L.A. Pruitt, *Nano Today* 1 (2006) 26.
- [41] L. Cheng, X. Xia, W. Yu, L.E. Scriven, W.W. Gerberich, *J. Polym. Sci., B: Polym. Phys.* 38 (2000) 10, doi:10.1002/(sici)1099-0488(20000101)38:1<10::aid-polb2>3.0.co;2-6.
- [42] A.C. Fischer-Cripps, *Nanoindentation*, 2nd Edition Springer-Verlag, 2004.
- [43] M. Oyen, R. Cook, *J. Mater. Res.* 18 (2003).
- [44] J.K. Deuschle, H.M. Deuschle, S. Enders, E. Arzt, *J. Mater. Res.* 24 (2009) 736.
- [45] X.-Y. Zhao, et al., *Polymer* 48 (2007) 6056.
- [46] S.J. Ahmadi, et al., *Compos. Sci. Technol.* 69 (2009) 2566.
- [47] M.J. Mayo, W.D. Nix, *Acta Metall.* 36 (1988) 2183.